# Climate–trait interactions dominate vegetation light use efficiency distributions across Chinae

Yujie Wang[1], Mingzhu He[23], Qian Zhang[4]

[1]School of Geography and Tourism, Qufu Normal University, Rizhao, 276826, China[2]~~Laboratory example, city, postal code, country~~

[2]Joint International Research Laboratory of Catastrophe Simulation and Systemic Risk Governance, Beijing Normal University, Zhuhai 519087, China

[3]School of National Safety and Emergency Management, Beijing Normal University, Zhuhai 519807, China

[4]College of Geodesy and Geomatics, Shandong University of Science and Technology, Qingdao 266590, China

*Correspondence to*: Mingzhu He (hemingzhu@bnu.edu.cn)

**Abstract.** Light use efficiency (LUE) is a key parameter in terrestrial carbon cycling, yet its spatial variability cannot be fully explained by climatic factors alone. Plant functional traits are expected to provide important physiological constraints on vegetation photosynthesis, but their roles and interactions with climatic drivers remain poorly understood, limiting the accuracy and improvement of carbon cycle modelling and projections. Here, we use eddy covariance observations from 29 flux sites, together with climate and trait data, to identify the drivers of LUE and map its spatiotemporal variations across China. Incorporating plant functional traits, including rooting depth, isohydricity, leaf nitrogen (N) content and specific leaf area (SLA), substantially improves the explanation of LUE spatial variability from 45% to 58%. The attribution analysis reveals that this improvement is mainly contributed by the nonlinear interactions between climatic factors and traits, accounting for 69.1% of the total importance and considerable exceeding the direct contributions from individual factors. Typically, the SLA-related interactions, particularly those involving rooting depth, temperature and vapor pressure deficit, largely explain tower-based LUE variations in China, suggesting that LUE is regulated by the coordination between vegetation carbon acquisition, soil water access and atmospheric constraints. Based on these findings, we generate a 1-km resolution annual LUE dataset for China spanning from 2003 to 2024. The regional LUE exhibits pronounced spatial heterogeneity but shows non-significant long-term trends during the study period. Our results emphasize that vegetation LUE distributions are mainly governed by the coupled climate–trait interactions, highlighting the need to represent trait-mediated environmental responses in terrestrial carbon cycle modelling.

## 1 Introduction

Terrestrial ecosystems absorb carbon dioxide from the atmosphere through vegetation photosynthesis, playing a vital role in regulating the global carbon cycle and mitigating climate change (Friedlingstein et al., 2023). Global terrestrial gross primary productivity (GPP), representing the total amount of carbon fixed by vegetation photosynthesis, has been estimated at approximately 123 ± 8 Pg C yr-1 based on flux tower observations (Beer et al., 2010). As a key parameter to estimate GPP,

light use efficiency (LUE) describes the efficiency of vegetation to convert light energy to produce biomass, and is a key variable for estimating gross primary productivity (GPP) (Yuan et al., 2010). In general, higher LUE values indicate stronger carbon assimilation capacity and more efficient light energy utilization, providing valuable information for understanding ecosystem carbon sequestration potential (Running et al., 2004). Existing LUE modeling frameworks, such as MOD17, primarily estimate ecosystem productivity by adjusting maximum LUE based on climatic stress functions (Pei et al., 2022). However, these approaches are largely environment-driven and may not fully capture the substantial variability of LUE across ecosystem types and spatial scales. (Heinsch et al., 2006; Zhao et al., 2005)

Recent studies have demonstrated that, in addition to climatic controls, plant functional traits play crucial roles in regulating ecosystem photosynthesis and carbon cycling (Yan et al., 2025). Plant functional traits are measurable morphological, physiological, and biochemical characteristics that reflect plant resource acquisition, growth, and adaptation strategies (Díaz et al., 2016; Wright et al., 2004). Commonly used traits include leaf nitrogen content (N), specific leaf area (SLA), rooting depth, and isohydricity, which characterize photosynthetic capacity, leaf economic strategies, belowground water acquisition, and stomatal regulation, respectively (Walker et al., 2014; Wright et al., 2004). Trait-based ecology provides a mechanistic bridge between environmental forcing and ecosystem functioning by linking plant physiological strategies to ecosystem-level processes (Díaz et al., 2016). As these traits directly influence vegetation physiology, they provide important biological constraints on ecosystem LUE (He et al., 2022; Yan et al., 2025). Increasing evidences show that incorporating traits can improve the accuracy of ecosystem productivity modeling and benefit the explanations of spatial variations in photosynthetic efficiency beyond climate-only approaches (He et al., 2022; Lin et al., 2021; Yan et al., 2025). These findings address that plant functional traits not only influence ecosystem carbon uptake directly, but also regulate ecosystem responses to environmental variability, making them key biological mechanisms manipulate the spatial variations in vegetation LUE.

Therefore, models relying solely on climatic drivers are potentially insufficient to fully capture the mechanisms governing LUE variability, and the exclusion of plant traits may introduce systematic biases in carbon fixation estimations. However, many previous studies have focused on site-level observations or specific ecosystem types (Garbulsky et al., 2010; He et al., 2022), whereas systematic evaluations across broad geographic regions and multiple vegetation types remain limited (Tang et al., 2020). In particular, the relative contributions of climatic factors and plant functional traits, as well as their potential interactions in regulating LUE, remain poorly quantified across different regions and vegetation types (Ali et al., 2015; Yan et al., 2025). Although plant functional traits vary substantially among plant functional types (PFTs), reflecting differences in woodiness, habitat type, and biogeographical context (Golivets et al., 2024), the extent to which these trait differences interact with climatic constraints to regulate ecosystem carbon-use efficiency remains unclear, particularly at regional scales.

The terrestrial ecosystems across China exhibit pronounced climatic gradients and high vegetation diversity, resulting in substantial heterogeneity in ecosystem structure and functioning (Piao et al., 2010). As one of the world's largest terrestrial carbon sink regions, China contributes substantially to global land carbon uptake (Friedlingstein et al., 2023). Because LUE is a key determinant of GPP, improving our understanding of the mechanisms governing LUE variability across China's diverse ecosystems is essential for reducing uncertainties in terrestrial carbon sink assessments and regional carbon budget evaluations.

Despite its importance, the mechanisms underlying LUE variability across China remain understudied, particularly regarding the synergistic functioning of climatic conditions and plant functional traits. In addition, most ecosystem classification schemes treat grasslands as a single plant functional type (PFT), thereby overlooking substantial differences between alpine meadows and temperate grasslands in hydrothermal conditions, resource-use strategies, and physiological adaptation mechanisms (Hao et al., 2021; Ni, 2004; Yang et al., 2021). Such simplifications may introduce additional uncertainties in regional-scale LUE estimation and carbon cycle assessments.

Based on these considerations, this study integrates eddy covariance observations from 29 flux sites, multi-source remote sensing data, and plant functional trait datasets from 2003 to 2024 to investigate the mechanisms regulating LUE spatial variability across China. Specifically, we identify the dominant drivers of LUE spatial distributions and quantify the relative contributions of climatic factors, plant functional traits, and their interactions. To achieve these objectives, random forest and SHAP analyses are employed. Based on those findings from site-level observations, we generate a 1-km resolution LUE map over China and systematically characterize its spatiotemporal patterns in the recent two decades. Overall, this study aims to disentangle the underlying mechanisms driving LUE variations incorporating multiple climatic factors and plant traits, explore their interactions across different PFTs, and improve our understanding of ecosystem carbon uptake processes at regional scales.

## 2 Materials and Methods

### 2.1 Study Area

The terrestrial ecosystems across China extend from approximately 18° to 53°N and encompass diverse climatic zones, ranging from the tropical and subtropical regions in the southeastern to the cold zones in the northeastern regions, from humid eastern to arid and semi-arid northwestern regions, and to the alpine climates of the Qinghai-Tibetan Plateau (QTP) (Duan et al., 2021; Hua et al., 2025-5-29). Driven by this diverse climate and complex topography, the PFTs over China exhibits distinct spatial patterns (Duan et al., 2021). Specifically, the forests in China transition from evergreen coniferous forests (ENF) and deciduous broad-leaved forests (DBF) in the northeastern to widespread DBF and mixed forests (MF) in northern and central China, and further to evergreen broad-leaved forests (EBF) in the subtropical and tropical regions located in the southeastern regions (Fig. 1a). Those forest ecosystems, covering about 23% of the land area in China, differ markedly in canopy structure and leaf functional traits, both of which strongly influence light interception and hence photosynthesis (Durand et al., 2022; He et al., 2022). Moreover, TG, OSH, SAV and WSA are primarily distributed in the northwestern China with relatively sparse vegetation cover. Whereas, the QTP is predominately characterized by AM. Characterized by the substantially different hydrothermal conditions and photosynthetic activities (Fang et al., 2024), those PFTs potentially show distinct LUE spatial variations over China.

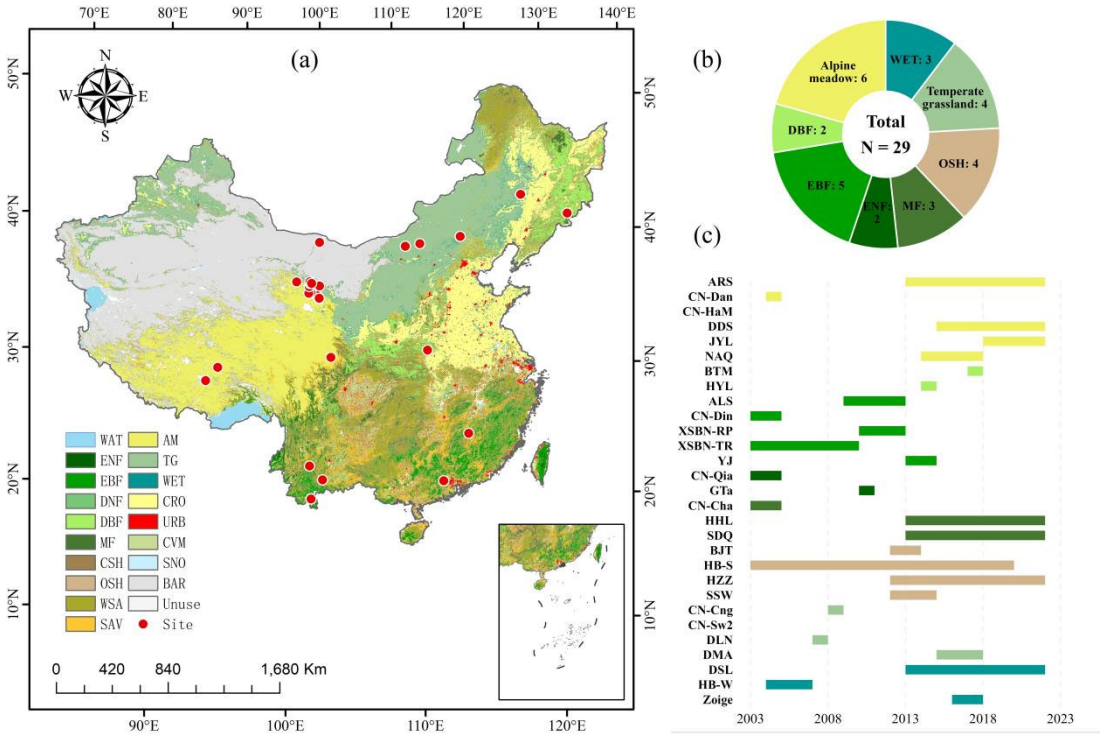


**Figure 1: The distributions of plant functional types (PFTs) and the examined flux tower sites in China. (a) The spatial distribution of PFTs in China. The vegetation map is obtained from the MODIS MCD12Q1 product with the IGBP classification scheme in 2024, and the red dots indicate the 29 flux tower sites used in this study. (b) The number of flux tower sites across different PFTs. (c) The time periods of observations from each flux tower site used in this study.**

### 2.2 Data sources and preprocessing

This study employs site-level eddy covariance observations from ChinaFLUX (Yu et al., 2006), FLUXNET2015 (Pastorello et al., 2020), and the Heihe River Basin dataset (Wang et al., 2025). To minimize the influence of anthropogenic management activities (i.e. irrigation and fertilization) on vegetation photosynthetic activities, cropland sites are excluded from analyses in this study. Therefore, a total number of 29 flux tower sites representing eight major PFTs is utilized, yielding 141 site-year observations, including AM (6 sites), TG (4 sites), EBF (5 sites), DBF (2 sites), MF, (3 sites), ENF (2 sites), WET (3 sites), and OSH (4 sites) (Table 1). These sites are distributed across a relatively wide range of hydrothermal conditions (Fig. 1), thereby capturing substantial environmental and vegetation variability across China's terrestrial ecosystems.

**Table 1: Summary of flux tower site characteristics**

| Site code | Latitude (°N) | Longitude (°E) | PFT | Time coverage |
|---|---|---|---|---|
| JYL | 37.8384 | 101.116 | Alpine meadow | 2018-2022 |
| ARS | 38.0473 | 100.4643 | Alpine meadow | 2013-2022 |

| | | | | |
|---|---|---|---|---|
| DDS | 38.0142 | 100.2421 | Alpine meadow | 2015-2022 |
| SDQ | 42.0012 | 101.1374 | MF | 2013-2022 |
| HHL | 41.9903 | 101.1335 | MF | 2013-2022 |
| GTa | 38.5333 | 100.25 | ENF | 2010-2011 |
| DSL | 38.8399 | 98.9406 | WET | 2013-2022 |
| HZZ | 38.7652 | 100.3186 | OSH | 2012-2022 |
| BJT | 38.915 | 100.3042 | OSH | 2012-2014 |
| SSW | 38.7892 | 100.4933 | OSH | 2015-2021 |
| HYL | 41.9932 | 101.1239 | DBF | 2014-2015 |
| CN-HaM | 38.6128 | 101.3128 | Alpine meadow | 2002-2004 |
| CN-Dan | 30.49728 | 91.06636 | Alpine meadow | 2004-2005 |
| CN-Sw2 | 41.77806 | 111.89722 | Temperate grassland | 2011 |
| CN-Cng | 44.5934 | 123.5092 | Temperate grassland | 2008-2009 |
| CN-Din | 23.1734 | 112.53436 | EBF | 2003-2005 |
| CN-Cha | 42.4025 | 128.09583 | MF | 2003-2005 |
| CN-Qia | 26.74141 | 115.05811 | ENF | 2003-2005 |
| HB-W | 37.6085 | 101.3273 | WET | 2004-2007 |
| NAQ | 31.6418 | 92.0153 | Alpine meadow | 2014-2018 |
| DLN | 42.0466 | 116.2836 | Temperate grassland | 2007-2008 |
| DMA | 41.643944 | 110.3284 | Temperate grassland | 2015-2018 |
| ALS | 24.5405 | 101.0278 | EBF | 2009-2013 |
| XSBN-RP | 21.9333 | 101.25 | EBF | 2010-2013 |
| XSBN-TR | 21.9275 | 101.2653 | EBF | 2003-2010 |
| YJ | 23.4778 | 102.1822 | EBF | 2013-2015 |
| BTM | 33.4997 | 111.9353 | DBF | 2017-2018 |
| Zoige | 33.10428 | 102.65147 | WET | 2016-2017 |
| HB-S | 37.66517 | 101.33117 | OSH | 2003-2020 |

To identify the climatic and biological controls on ecosystem LUE, variables in three categories, including PFT, climatic variables, and plant functional traits (Table 2), are utilized in this study. PFT data is obtained from the MODIS MCD12Q1 land-cover product with the IGBP classification scheme, which provides annual land-cover maps at a spatial resolution of 500 m. Annual PFT maps from 2003 to 2024 were used to account for potential land-cover changes during the study period. To better distinguish climatic and ecological differences among grassland ecosystems, grasslands are further classified into temperate grasslands (TG) and alpine meadows (AM) according to the boundary of the Qinghai–Tibet Plateau.

**Table 2: Summary of predictor datasets**

| Variable | Dataset | Spatial resolution | Temporal resolution | Period |
|---|---|---|---|---|
| PFT | MODIS MCD12Q1 | 500 m | Annual | 2003–2024 |
| TA | China 1-km Temperature Dataset | 1 km | Monthly | 2003–2024 |
| SWC | China Soil Moisture Dataset | 1 km | Daily | 2003–2024 |
| VPD | ERA5-Land-derived | 0.1° | Monthly | 2003–2024 |
| N | China Plant Trait Dataset | 1 km | Static | - |
| SLA | China Plant Trait Dataset | 1 km | Static | - |
| Isohydricity | Konings & Gentine | 0.25° | Static | - |
| Rooting depth | Lusk et al. | 1 km | Static | - |

Climatic variables including air temperature (TA), soil water content (SWC), and vapor pressure deficit (VPD) are incorporated as the climate controls for LUE spatial variations. TA is obtained from the China 1-km Resolution Monthly Average Air Temperature Dataset, which provides monthly observations at a spatial resolution of 1 km from 2003 onward (Peng et al., 2019). Soil water content (SWC) is derived from the China 1-km Resolution Daily All-Day Surface Soil Moisture Dataset, which provides daily observations at a spatial resolution of 1 km (Song et al., 2022). Vapor pressure deficit (VPD) is calculated using the Tetens formulation (Allen et al., 1998) based on monthly 2-m air temperature and dew point temperature from ERA5-Land, which provides meteorological variables at a spatial resolution of approximately 0.1° (~9 km) (Muñoz-Sabater et al., 2021)

$$e_s = 0.6108 \times exp\left(\frac{17.27 \times t_{2m}}{t_{2m}+237.3}\right), \quad (1)$$

$$\mathrm{e_a} = 0.6108 \times \exp\left(\frac{17.27 \times \mathrm{d_{2m}}}{\mathrm{d_{2m}}+237.3}\right), \quad (2)$$

$$\mathrm{VPD} = \mathrm{e_s} - \mathrm{e_a}, \quad (3)$$

Four plant functional traits are selected to represent key characteristics of plant resource acquisition and water-use strategies, including leaf nitrogen (N) content, specific leaf area (SLA), isohydricity, and rooting depth. Leaf N and SLA are obtained from a high-resolution plant trait dataset for China at 1-km spatial resolution (An et al., 2024). Isohydricity is obtained from the global isohydricity dataset developed by Konings and Gentine (2017), with an original spatial resolution of 0.25°. Rooting depth is derived from a global plant trait dataset based on crowdsourced biodiversity observations, providing community-weighted mean rooting depth at 1-km resolution (Lusk et al., 2026). These predictors are selected according to their complementary physiological roles in regulating ecosystem LUE and the availability of spatially continuous datasets for nationwide analysis. Air temperature (TA) represents thermal constraints on photosynthetic processes, as photosynthetic activity exhibits nonlinear responses to temperature, with declines occurring beyond optimal thermal conditions (Duffy et al., 2021). Vapor pressure deficit (VPD) represents atmospheric water demand, which can induce stomatal closure and restrict photosynthetic carbon uptake under strong atmospheric dryness (Grossiord et al., 2020; Novick et al., 2024). Soil water content (SWC) represents soil water supply and complements VPD by distinguishing soil water limitations from atmospheric water demand. SWC can directly constrain photosynthesis and interact with atmospheric dryness to regulate ecosystem carbon uptake (Humphrey et al., 2021). At the leaf level, nitrogen content (N) is closely associated with photosynthetic biochemical capacity, whereas specific leaf area (SLA) reflects leaf construction and resource-acquisition strategies along the leaf economics spectrum (Evans, 1989; Walker et al., 2014). At the whole-plant level, rooting depth reflects the potential capacity to access water in deeper soil layers (Fan et al., 2017), while isohydricity characterizes variation in stomatal regulation strategies under changing water availability (Konings and Gentine, 2017; Tardieu and Simonneau, 1998). In addition, PFT is included to represent broad differences in vegetation structure, phenology, and ecosystem functioning that are not fully captured by individual plant traits (Díaz et al., 2016). Collectively, these predictors represent complementary climatic, physiological, and vegetation-level controls on LUE, and are selected for analyses in this study.

Solar-induced fluorescence (SIF) data are obtained from the global spatially contiguous SIF (CSIF) dataset (Zhang et al., 2018), which covers the period 2000–2022. SIF yield is calculated as the ratio of SIF to absorbed photosynthetically active radiation (APAR)(Yang et al., 2015), with APAR is estimated as the product of photosynthetically active radiation (PAR) and the fraction of absorbed photosynthetically active radiation (FPAR). FPAR is obtained from the MODIS MOD15A2H.061 product(Myneni et al., 2021), and PAR is obtained from the MODIS MCD18C2.062 product(Wang, 2025).

To ensure spatial comparability among datasets with different native spatial resolutions, all the datasets are resampled to a common 1-km grid using bilinear interpolation and reprojected using WGS84 coordinate system. To match the annual flux tower–based LUE observations, both daily and monthly datasets are aggregated or averaged to annual values, generating a continuous time series from 2003 to 2024. All the explanatory variables are then standardized using Z-score normalization, defined as follows:

$$Z = \frac{x-\mu}{\sigma}, \quad (4)$$

Where x is the original value, μ is the mean, and σ is the standard deviation.

### 2.3 Light use efficiency (LUE) estimation

According to the LUE framework, it is calculated as follows (Monteith, 1972):

$$\mathrm{LUE} = \frac{\mathrm{GPP}}{\mathrm{FPAR}\times\mathrm{PAR}} = \frac{\mathrm{GPP}}{\mathrm{FPAR}\times\mathrm{SW}\times 0.45}, \quad (5)$$

Gross primary productivity (GPP) is obtained from flux tower observations, with units of g C $m^{-2}$. FPAR is the fraction of canopy absorbed photosynthetically active radiation, and PAR is photosynthetically active radiation, which could be estimated as shortwave radiation (SW) multiply by 0.45 (He et al., 2022). In this study, FPAR is obtained from the MODIS FPAR product (MOD15A2H.061) (Myneni et al., 2021), whereas SW was obtained from flux tower radiation measurements. The resulting light use efficiency (LUE) is expressed in units of g C $MJ^{-1}$.

### 2.4 LUE driver analysis and spatial extrapolation

In this study, Random Forest (RF), a tree-based ensemble learning algorithm capable of capturing nonlinear relationships and complex interactions among variables (Breiman, 2001), is used to investigate the underlying mechanisms driving LUE variations across China. The RF model is trained using a repeated site-based random partitioning approach. In each iteration, approximately two-thirds of the flux tower sites are randomly selected for model training, while data from all the available flux tower sites are used for model testing. Model performance is hence assessed using the coefficient of determination ($R^2$) and root mean square error (RMSE). This procedure is repeated 50 times, and the results are shown as mean ± standard deviation.~~Model performance is evaluated using a repeated site-based cross-validation approach. For each iteration, approximately two-thirds of the flux tower sites are randomly selected as the training set, while the remaining sites are reserved for validation. Each process is repeated 50 times using different random site partitions, and model performance is assessed on the independent validation sites.~~ To reduce overfitting, the number of trees (ntree) was set to 500, the number of variables randomly sampled at each split (mtry) was set to 4, and the maximum number of terminal nodes (maxnodes) was set to 16. To specify the contributions of plant functional traits to LUE variability, two comparable RF models are run. The first RF model (full model) incorporates all the explanatory variables including PFTs, climatic and trait data. Whereas, the second one (climate-only model) only employs the PFT and climatic variations to modulate LUE variations. Any differences between those two models indicate the contributions of plant functional traits to explain LUE variations.

SHapley Additive exPlanations (SHAP) is applied to interpret the results from the trained RF model (Lundberg and Lee, 2017). SHAP values exhibit the contributions of each predictor to model outputs and provide a consistent framework for explaining complex machine-learning models. Global importance rankings, marginal response patterns, and pairwise interaction effects are further analyzed based on SHAP values to identify the dominant controls on LUE across China's terrestrial ecosystems. Based on the identified climate-trait controls, the annual 1-km LUE maps are generated through running the RF model with all the explanatory variables across China from 2003 to 2024.

## 3 Results

### 3.1 Variability of tower-based LUE across ecosystems

Through tower-based observations, LUE shows substantial spatial variabilities across China's terrestrial ecosystems. Specifically, LUE ranges from 0.064 to 2.98 g C $MJ^{-1}$, with a mean value of 0.88 ± 0.62 g C $MJ^{-1}$ across the selected 29 flux tower sites (Fig. 2a). Moreover, site-level LUE reveals right-skewed distributions, with the majority of observation-based values concentrated between 0.50 and 1.50 g C $MJ^{-1}$ and a long tail toward high values, indicating pronounced spatial heterogeneity in LUE distributions over China. Such spatial variability is also revealed by PFTs, indicating the highest LUE values for EBF (1.41 ± 0.58 g C $MJ^{-1}$), in comparisons with the significantly lowest values (0.46 ± 0.22 g C $MJ^{-1}$) for AM. LUE in WET also showed substantial variability (1.18 ± 0.87 g C $MJ^{-1}$), possibly reflecting the broad environmental gradients covered by the corresponding site-level observations (Fig. 1).However, LUE is generally stable in ENF (1.40 ± 0.067 g C $MJ^{-1}$), which may also be contributed by the relatively few observations (Fig. 2b).

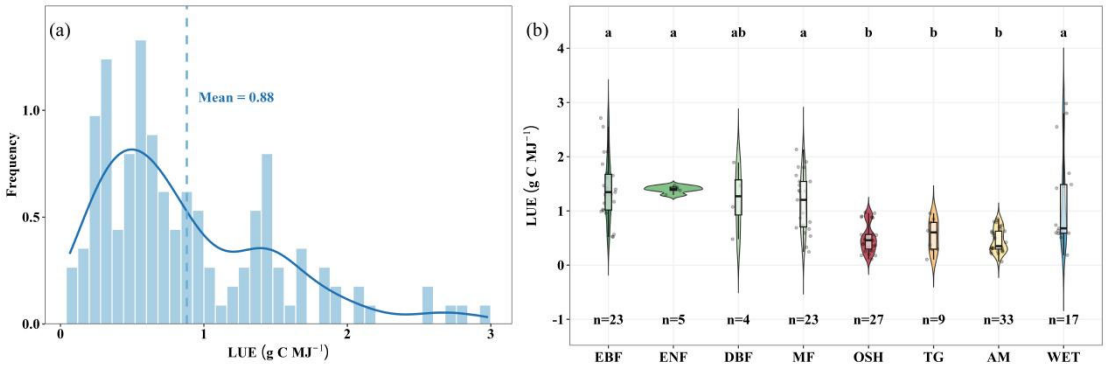


**Figure 2: The distributions of LUE over the 29 flux tower sites in China. (a) The histogram of LUE across the examined 29 flux tower sites. (b) The LUE variations among different PFTs. One-way ANOVA analysis is performed to identify the significant ($p < 0.05$) differences of LUE among different PFTs with noting different letters on the top of each violin. The number of site-years for each PFT is also stated.**

Furthermore, forest ecosystems consistently show higher LUE values and narrower variations, indicating that forests generally grow in more favorable hydrothermal conditions and exhibit greater and more stable photosynthetic efficiency. In contrast, non-forests ecosystems, including TG, AM and OSH, show lower LUE values but stronger site-specific variabilities, indicating that the sparse vegetation cover could reduce the photosynthetic efficiency, as well as the limited hydrothermal conditions. Specifically, the particularly low LUE values in AM (0.46 ± 0.22 g C $MJ^{-1}$) underscores the vegetation growth constraints imposed by low temperature and hence short growing season in QTP (Shen et al., 2022). Whereas, the relatively low LUE values in TG and OSH could probably be explained by water limitations in the northwestern regions. As a result, LUE shows distinct variations across different PFTs and regions, raising the need to investigate its dominant drivers over China.

### 3.2 The driving mechanisms for LUE variations

For better understanding of LUE variations, we run two RF models to disentangle the roles of plant functional traits on LUE variations. One RF model is the full model incorporating all the explanatory variables, and the other is the climate-only model, which is forced by PFT and climatic variables (i.e. TA, VPD, SWC). The differences in the performance between these two models characterize the contributions gained from plant functional traits, as well as their interactions with climatic variables. The full model shows high performance to simulate the variations of observation-based LUE with R2 value of 0.58 and RMSE value of 0.39 g C $MJ^{-1}$ (Fig. 3). Notably, it obviously outperforms the climate-only model, indicating approximately 13% higher R2 and 6% lower RMSE values. This finding underscores the importance of including plant functional traits in LUE simulations and hence vegetation photosynthesis modeling.

Across the 50 repeated iterations, the full model achieves a mean $R^2$ of 0.924 ± 0.011 and an RMSE of 0.165 ± 0.017 g C $MJ^{-1}$ from the training processes. When the trained model is applied to all available flux tower sites, the mean $R^2$ and RMSE are 0.583 ± 0.123 and 0.393 ± 0.060 g C $MJ^{-1}$, respectively (Fig. 3). The climate-only model shows relatively lower performance, with a mean $R^2$ of 0.842 ± 0.025 and an RMSE of 0.237 ± 0.028 g C $MJ^{-1}$ from the training processes, and 0.454 ± 0.176 and 0.449 ± 0.070 g C $MJ^{-1}$ across all available sites, respectively. Notably, the full model outperforms the climate-only model with a higher $R^2$ by 0.129 and lower RMSE by approximately 12.5% based on the results from all the available sites. These results indicate that incorporating plant functional traits improves the overall representation of LUE variability across the available flux tower sites, highlighting the importance of plant functional traits in LUE simulations and vegetation photosynthesis modeling.

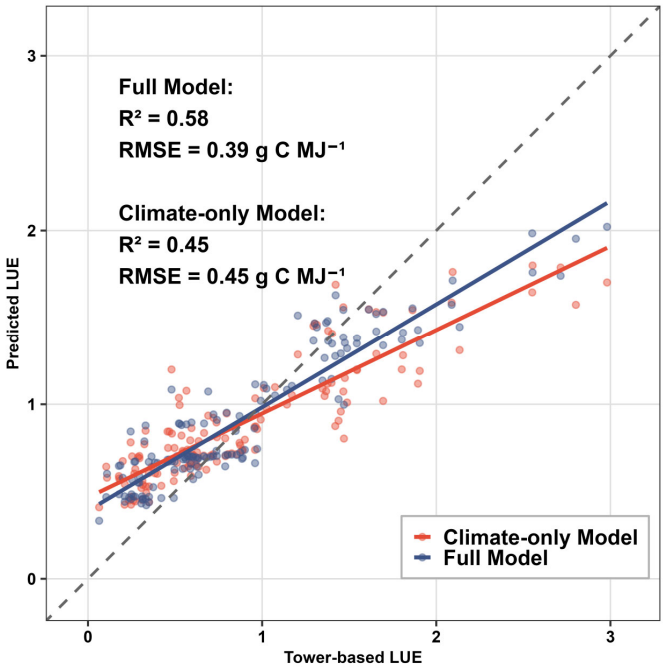


**Figure 3: Model performance of LUE simulations. Two random forest models are run here, one is the full model with using all the variables as inputs, and the other one is the climate-only model, which only uses the climatic factors and plant functional types as forcings. The predicted LUE from these two models are compared with the flux tower-based LUE estimates.**

To further identify the mechanisms underlying LUE variability, we incorporate SHAP attribution analysis with the full RF model to quantify the relative importance of different factors to drive LUE variations (Fig. 4). The interactions between SLA and rooting depth emerge as the most important factor influencing LUE variations across the examined 29 flux tower sites (Fig. 4). Such interactions reveal the coordination between vegetation light capture and soil water accessibility. That is, SLA is closely linked to the leaf economic spectrum, light interception, and photosynthetic capacity (Reich, 2014; Wright et al., 2004), and it emerged as the third important factor driving spatial variations in LUE (Fig. 4). Deep-rooted vegetation could access water in deep soil and maintain stomatal opening during dry periods, thereby buffering water stress and sustaining photosynthesis (Fan et al., 2017; Lusk et al., 2026). Accordingly, high SLA with shallow roots, low SLA with deep roots, and low SLA with shallow roots all restrict LUE through limited water or light acquisition or both (Fig. 5a). Optimally, high SLA interacts with deep roots to promote LUE, owing to efficient light acquisition and enough soil water supply (Fan et al., 2017; Lusk et al., 2026; Reich, 2014; Wright et al., 2004). However, very high SLA might also depress LUE under stronger environmental stress, particularly when water limitation or high VPD offsets the photosynthetic benefits of rapid light acquisition (Fig. 5a, c), indicating that generally thin and short-lived leaves reduce the efficiency of light interception.

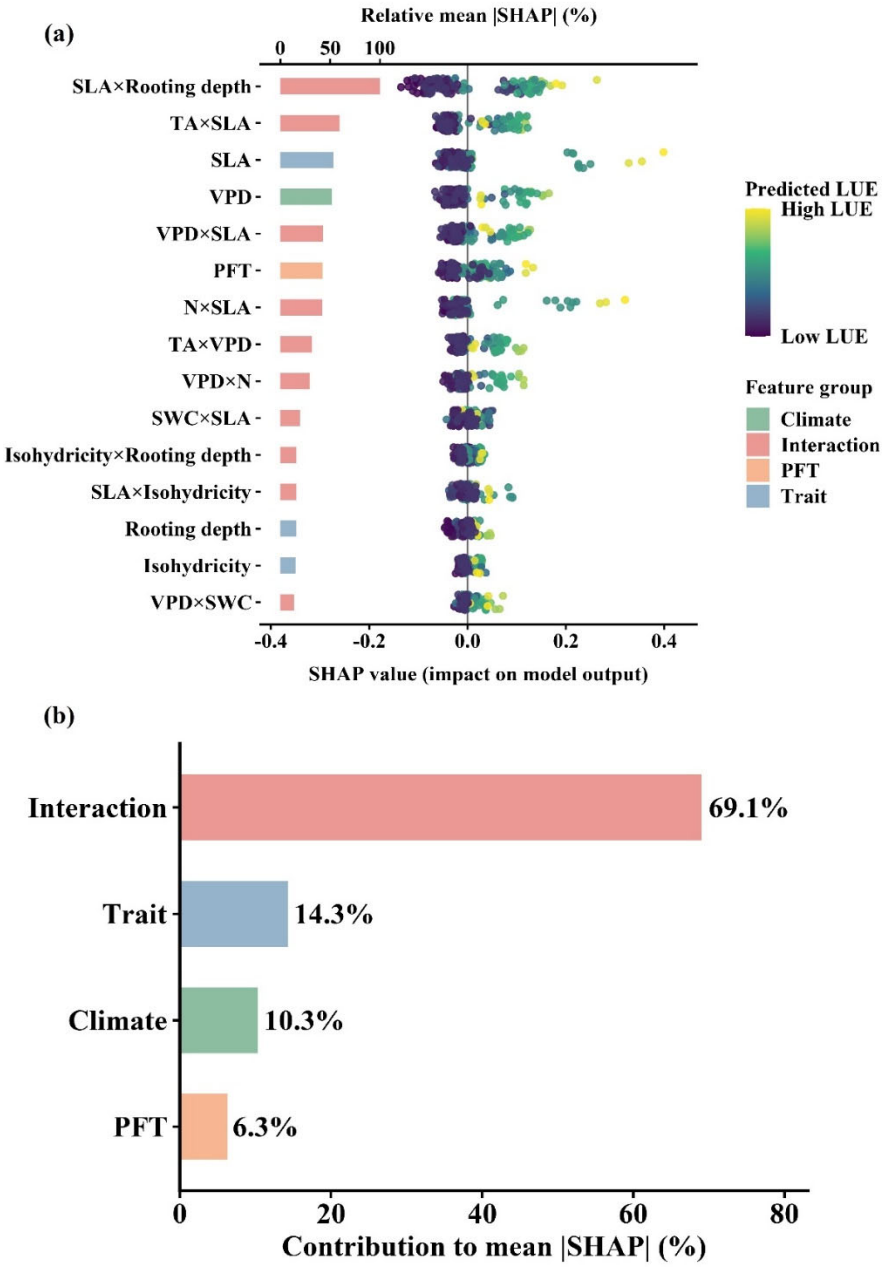


255 **Figure 4: The importance of multiple climate and trait factors to light-use efficiency (LUE) variations in China. (a) Bee-swarm plot of SHAP values of PFT, different climatic, trait factors and their interactions are also shown here. (b) Group-level contributions of interaction, trait, climate, and PFT factors to mean |SHAP| (%).**

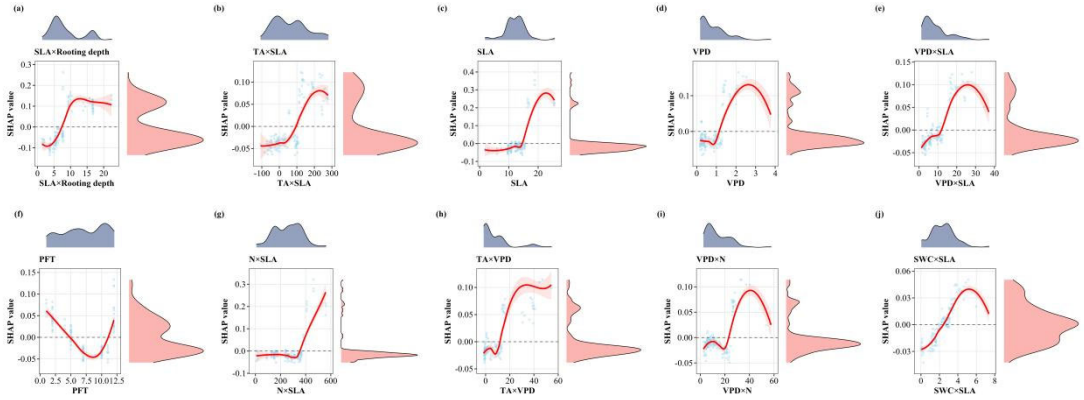


**Figure 5: The dependency plots of light use efficiency (LUE) on the top ten driving factors in China. Each plot illustrates the relationships between a single factor (x-axis) and its SHAP value (y-axis), representing its marginal contributions to predict LUE variations. The red line indicates the locally weighted scatterplot smoothing (LOWESS) curve that reveals general trends. The blue histogram above the plot shows the frequency distribution of each factor, while the red histogram to the right shows the distribution of SHAP values.**

Moreover, the interactions between SLA and TA rank the second importance to explain LUE variations (Fig. 4), suggesting the functional coordination of leaf economics and thermal conditions. Under favorable thermal conditions, high SLA could promote photosynthetic efficiency (Fig. 5b) and support rapid carbon acquisition. However, when temperature increases beyond the optimal range, the positive effect may weaken due to excessive heat may reduce photosynthetic efficiency as high TA leads to photosynthetic enzyme inactivation. This finding indicates that SLA does not regulate LUE independently; instead, its effect is expressed through a temperature-dependent response of leaf photosynthetic activity.

VPD, indicating the atmospheric water demand, shows pronounced nonlinear effects on LUE variations (Fig. 4, 5d). The response curve indicated a unimodal pattern, with LUE reaching its highest contribution at intermediate VPD levels (approximately 2.00~3.00 kPa) and declining under both low and high VPD conditions (Fig. 5d). Low VPD may occur under cloudy or radiation-limited conditions, which can restrict photosynthesis and reduce LUE. However, high atmospheric water demand could lead to stomatal closure and reduces the photosynthetic capacity (Grossiord et al., 2020; Novick et al., 2016, 2024), causing LUE to decrease. This nonlinear response of LUE to VPD has profound implications for land surface model improvements, as some current models just utilizing linear VPD parameterizations may introduce uncertainties in carbon fixation simulations. Furthermore, the skewed distributions of both VPD and the corresponding SHAP values manifest that most terrestrial ecosystems in China experience VPD below the optimal threshold for photosynthesis.

Furthermore, the above two important factors, SLA and VPD, interact with each other to exerts the fifth importance regulating LUE variations (Fig. 4), illustrating that atmospheric dryness modifies the effect of leaf economic strategy on LUE. The nonlinear response of this interaction suggests that SLA-related carbon acquisition is enhanced under low-to-moderate VPD,

but becomes constrained when VPD continues to increase (Fig. 5e). Under high VPD, the advantage of vegetation with high SLA may be weakened because partial stomatal closure restrict photosynthetic carbon gain. Vegetation with high SLA could achieve high LUE only when atmospheric water demand remains within a suitable range. Thus, VPD × SLA captures an important ecological trade-off: traits that promote rapid carbon acquisition can increase LUE under favorable atmospheric moisture conditions, but may become vulnerable under atmospheric drought, which has been increasingly recognized as a key mechanism regulating ecosystem productivity under climate change (Grossiord et al., 2020; Novick et al., 2016). Such similar trade-off is shown for SWC, exhibiting that LUE of vegetation with strong light interception is stimulated under favorable soil water conditions (Fig. 5j). High investments of assimilated carbon to leaf might suppress LUE due to inefficient light capture, whereas, much soil water may restrict vegetation root respiration and even lead to vegetation death under flooding. Alternatively, the interactions between SLA and leaf N content, revealing the N allocation efficiency, impose straightforward stimulations on LUE under relatively high SLA and high leaf N (Fig. 5g). Leaf N is necessary for photosynthetic enzyme constitutions (Evans, 1989; Rogers et al., 2017), potentially enhancing LUE with increasing content. Collectively, the important leaf economic trait, SLA interacts with rooting depth, VPD, SWC and N to exert multifunctional effects on LUE variations across the investigated 29 flux tower sites, illustrating the synergistically coupling between plant traits and climate. The biome specific differences in canopy structure, phenology, and carbon assimilation strategy, which are revealed by PFT, provide direct contributions to influence LUE variations (Fig. 4. 5f). However, compared with some carbon cycle models considering PFT as the dominant classifier for LUE (Heinsch et al., 2006; Running et al., 2004), this study indicates that vegetation LUE is more directly shaped by the interactions between plant traits and climatic and hydrological constraints. Nevertheless, this finding is consistent with previous studies showing that ecosystem differences in LUE are closely related to vegetation physiological characteristics, resource-use strategies, and environmental gradients rather than biome classification alone (Garbulsky et al., 2010; Madani et al., 2017).

It is worth to note that isohydricity, representing the stomatal regulation strategy constrained by water, appears to be one of the key traits affecting LUE variations, not only through its interactions with rooting depth and SLA, but also by itself (Fig. 4). Anisohydric vegetation (low isohydricity) tends to sustain stomatal conductance and maintain carbon uptake despite water stress (Konings and Gentine, 2017; Tardieu and Simonneau, 1998), thereby potentially enhancing LUE. Conversely, isohydric ecosystems show strict regulations on stomatal conductance and reduce stomatal opening under water stress (Konings and Gentine, 2017; Tardieu and Simonneau, 1998). When interacting with deep roots, these ecosystems achieve high LUE values to promote carbon uptake.

As a result, the nonlinear interactions between plant traits and climatic factors dominate LUE variations, accounting for 69.1% of the contributions (Fig. 4). This result indicate that these factors are synergistically collaborated to regulate vegetation carbon uptake efficiency, rather than single controls. Notably, plant functional traits alone account for 14.3% of the total importance, and exceed the contributions of climatic variables (10.3%), underscoring the importance of plant functional traits to provide unique controls on LUE beyond which captured by climate conditions alone (Madani et al., 2017). These findings are consistent with trait-based ecological theory, which emphasizes that plant functional traits regulate resource acquisition, allocation, and

utilization, thereby constraining photosynthetic efficiency (Reich, 2014; Wright et al., 2004). Overall, our results highlight that current carbon cycle models that treat climate and traits as independent forcing will systematically misinterpret LUE variations (Rogers et al., 2017; Verheijen et al., 2015) and introduce uncertainties to project vegetation responses to environmental change. Instead, the explicit incorporations of climate-trait coupling, especially the coupling of SLA with rooting depth, TA and VPD, show high potential to accurately capture the dynamics of vegetation photosynthetic efficiency over Chinese ecosystems (Matheny et al., 2017).

### 3.3 Regional mapping of LUE across China

According to the above detected mechanisms driving LUE variations based on flux tower observations, we map LUE regionally across Chinese ecosystems during the time period of 2003 to 2024 (Fig. 6a). The regional LUE estimates reveal pronounced spatial heterogeneity across China during 2003–2024, showing the mean LUE of 1.13 ± 0.20 g C $MJ^{-1}$ (Fig. 6a). Generally, LUE shows low values in the QTP and northwest regions, where vegetation growth is mostly limited by low temperature, short growing season, water stress, and so on. In contrast, in the Sichuan Basin and northeast China, LUE shows relatively high values (> 1.50 g C $MJ^{-1}$). Inter-mediate LUE values (1.00~1.50 g C $MJ^{-1}$) could be achieved in the middle to southeast China (Fig. 6a). Therefore, LUE generally shows west-to-east increasing patterns in China during the study period, broadly corresponding to thermal and moisture gradients. Ecosystems with relatively high LUE are generally located in warm and humid areas, whereas low-LUE ecosystems are mainly associated with water- and/or temperature-limited regions, or even nutrients-limited regions.

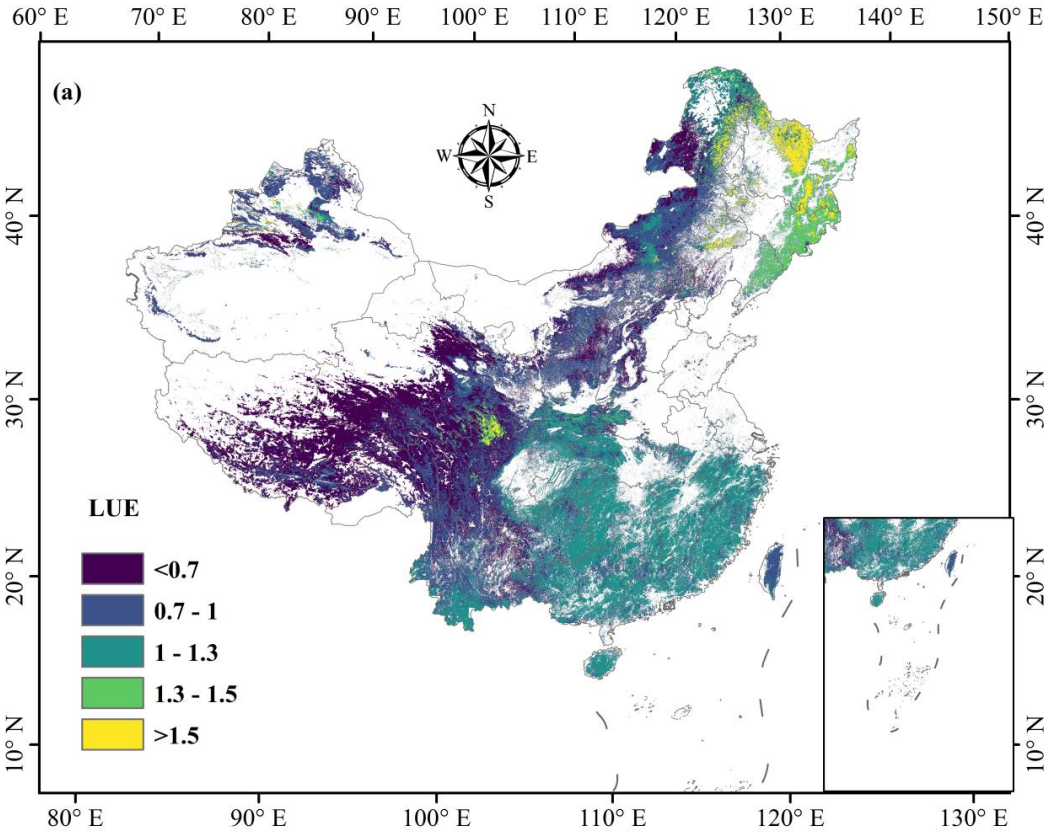
(a)
60° E
70° E
80° E
90° E
100° E
110° E
120° E
130° E
140° E
150° E
40° N
30° N
20° N
10° N
N
W
E
S
LUE
<0.7
0.7 - 1
1 - 1.3
1.3 - 1.5
>1.5

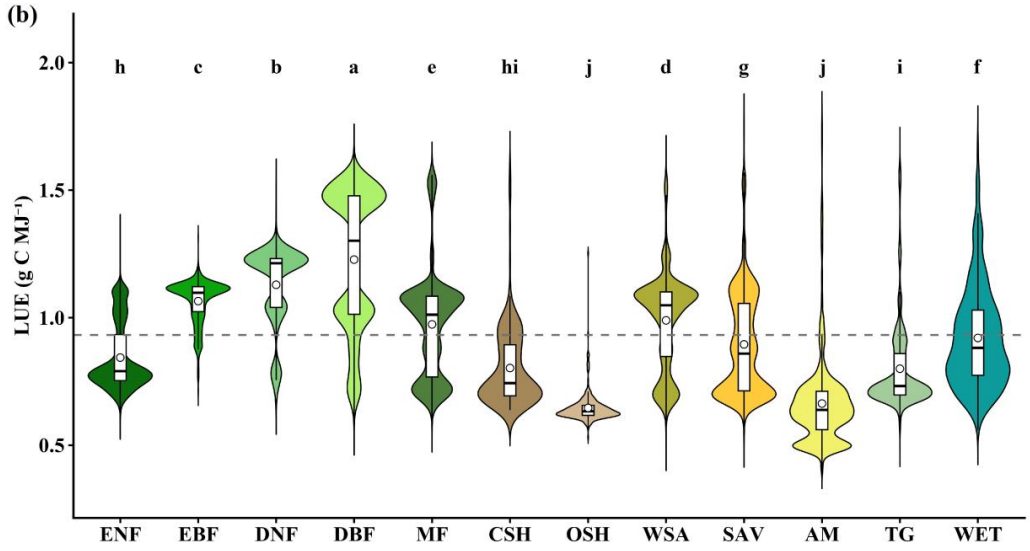
(b)
LUE (g C MJ⁻¹)
2.0
1.5
1.0
0.5
h
c
b
a
e
hi
j
d
g
j
i
f
ENF
EBF
DNF
DBF
MF
CSH
OSH
WSA
SAV
AM
TG
WET

**Figure 6: Spatial distributions of light use efficiency (LUE) across China. (a) Spatial pattern of LUE across China derived from upscaling flux tower–based measurements; (b) The difference of LUE over major plant functional types (PFTs) in China.**

Moreover, LUE distributions exhibit altitudinal gradients, shows decreasing values with increasing elevation (Fig. 6a). Ecosystems located in the lowland regions typically indicate LUE values of about 1.00~1.50 g C $MJ^{-1}$, whereas, ecosystems in the high-elevated regions reveal LUE values below 0.70 g C $MJ^{-1}$. This pattern aligns with the findings from previous studies that temperature limitation, short growing-season length and physiological stress at high elevations constrain vegetation photosynthetic efficiency (Ganjurjav et al., 2016; Mei et al., 2021; Xie et al., 2024).

Significant differences are also shown in LUE among different PFTs (Fig. 6b). Although LUE directly links with vegetation physiological characteristics and resource-use strategies (Garbulsky et al., 2010; Madani et al., 2017), PFT serves as another important factor to distinguish LUE over different regions. Specifically, DBF exhibits the highest mean LUE values (1.23 ± 0.28 g C $MJ^{-1}$), whereas OSH (0.65 ± 0.06 g C $MJ^{-1}$) and AM (0.66 ± 0.18 g C $MJ^{-1}$) generally show lower values among all the PFTs. Furthermore, forest ecosystems, including ENF, EBF, DNF, DBF and MF, overall show relatively high LUE with narrow spatial variations. In comparisons, non-forest ecosystems display lower LUE values and more fluctuated distributions. The regional LUE patterns are mostly consistent with the previous investigations. Similar LUE values of 0.30~1.80 g C $MJ^{-1}$ were reported previously with using MODIS and tower-based data (Yuan et al., 2007). The relatively higher LUE values for DBF than EBF and ENF were also revealed by (Zhang et al., 2017) over Chinese ecosystems. Despite such consistency, we highlight the importance of plant traits to explain LUE variations, which are not included in previous studies.

The relatively high LUE in northeastern China may be partly associated with regional differences in leaf N content. Our analysis indicates that leaf N content is generally higher in northeastern China than the rest of China. Leaf nitrogen plays an important role in photosynthesis, as it is an essential component of photosynthetic enzymes and proteins and is closely associated with photosynthetic biochemical capacity (Evans, 1989; Walker et al., 2014). Thus, higher leaf N content may support greater photosynthetic capacity and potentially contribute to the relatively high LUE observed in northeastern China.

Despite substantial spatial heterogeneity, the regional LUE shows small fluctuations from 2003 to 2024, revealing a non-significant temporal trend in the recent two decades (Fig. 7a). Regionally, approximately 31.0% of the study area exhibits significant changes in LUE, including significant LUE increases across 16.7% and significant decreases across 14.4% of the study domain (Fig. 7b). Regions with increasing LUE from 2003 to 2024 are mainly distributed in parts of eastern Inner Mongolia, the eastern QTP, and parts of the Loess Plateau, suggesting increasingly favorable conditions for ecosystem carbon uptake in these regions. In contrast, decreasing trends are concentrated in the Hengduan Mountains, southern China, and northern Northeast China, inferring exacerbated constraints on ecosystem photosynthetic efficiency.

The significant LUE declines in parts of southern China may be associated with the nonlinear responses of LUE to atmospheric moisture conditions. Our additional analysis shows that areas exhibiting significant LUE declines across China are characterized by relatively low VPD, with a mean of 0.442 kPa and a 10th–90th percentile range of 0.177–0.614 kPa. These values largely fall within the range associated with negative VPD SHAP contributions in our RF model (below approximately

1.2 kPa; Fig. 5d), suggesting that low-VPD conditions are associated with lower model-predicted LUE. Previous studies highlight the important role of VPD in regulating ecosystem LUE and photosynthetic processes (Fei et al., 2019; Grossiord et al., 2020). In addition, widespread warming occurs across southeastern China during 2003–2024, while SWC exhibits spatially heterogeneous changes, including decreases in some areas. Photosynthetic carbon uptake can be constrained when temperatures exceed ecosystem-specific optima (Duffy et al., 2021), whereas reduced soil water availability can limit photosynthesis through stomatal and non-stomatal processes (Zhou et al., 2015). Together, these findings suggest that the LUE declines may reflect the combined influence of atmospheric moisture conditions, temperature, and soil water availability, although the relative contributions of individual factors remain uncertain. However, LUE over about two-thirds of the regions in China exhibit non-significant trend in the recent two decades, resulting in overall non-significant temporal variabilities across China (Fig. 7a). This result suggests that the carbon assimilation efficiency could be treated as plant trait. Moreover, the non-significant temporal trend implies that potential positive effects gained from climate warming and elevated atmospheric $CO_2$ on photosynthesis may be partially offset by exacerbating environmental constraints, particularly those associated with atmospheric dryness and water limitation (Grossiord et al., 2020; Novick et al., 2016).

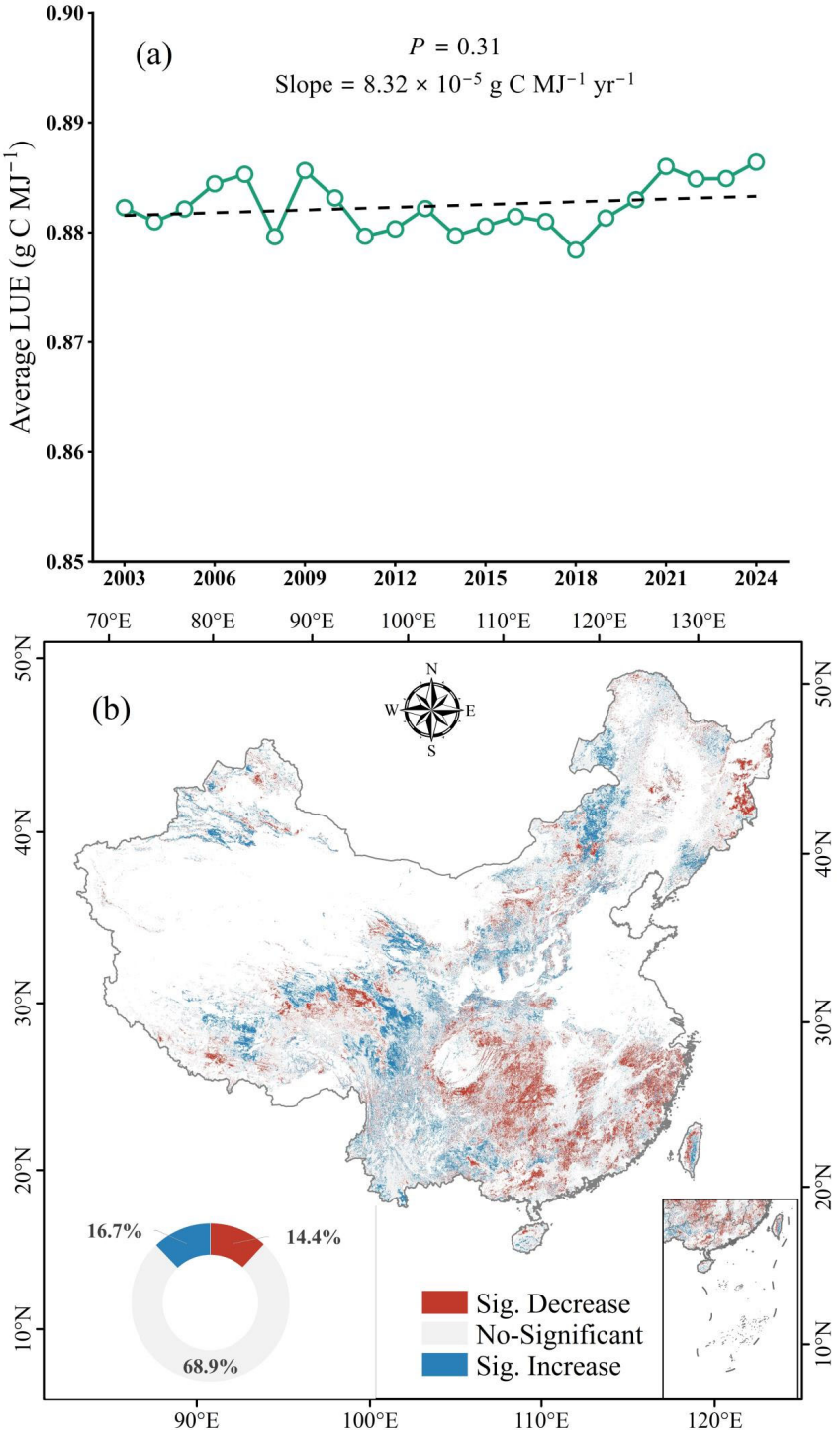
(a)
P = 0.31
Slope = 8.32 × 10−5 g C MJ−1 yr−1
Average LUE (g C MJ−1)
0.90
0.89
0.88
0.87
0.86
0.85
2003
2006
2009
2012
2015
2018
2021
2024
(b)
N
W
E
S
70°E
80°E
90°E
100°E
110°E
120°E
130°E
50°N
40°N
30°N
20°N
10°N
16.7%
14.4%
68.9%
Sig. Decrease
No-Significant
Sig. Increase

380

**Figure 7: Spatiotemporal trends of annual mean light use efficiency (LUE) in China from 2003 to 2024. (a) interannual variability of national mean annual LUE during 2003–2024.; (b) Spatial trends of annual mean LUE across terrestrial ecosystems in China.**

To further address the robustness of the estimated LUE, we compare its multi-year mean spatial consistencies with SIF yield over 2003–2020. Since LUE and SIF yield have different units, the normalized values (Z-score) of these two variables are used for comparisons. The strong and significant positive spatial correlations are shown here ($r = 0.563$, $P < 0.001$; Fig.8), indicating broadly consistent spatial distributions between these two datasets, and implying the reliability of the estimated LUE in this study.

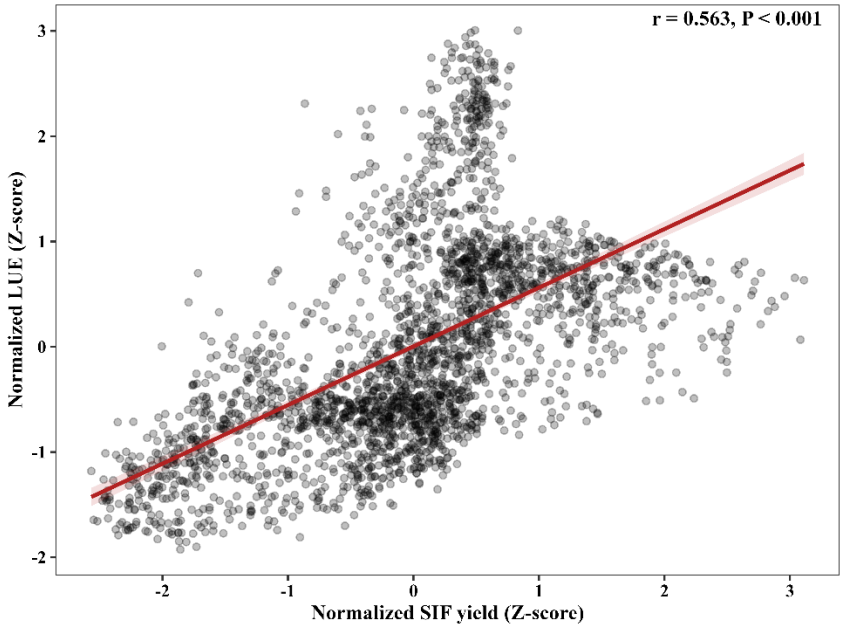


**Figure 8: Spatial relationship between multi-year mean normalized LUE and SIF yield across China during 2003–2020.** The red line represents the ordinary least squares (OLS) linear regression fit, and the shaded area indicates the 95% confidence interval.

### 3.4 Uncertainties and implications for carbon-cycle assessment

Several uncertainties should be noted in this study. Previous studies showed that incorporating a broader spectrum of plant functional traits can improve the representation of ecosystem physiological processes and reduce uncertainty in carbon-cycle modelling (Van Bodegom et al., 2012). Although plant functional traits substantially improve the explanations of LUE spatial variability, the trait representation in this study remains incomplete. Only four traits, including leaf N content, SLA, rooting depth, and isohydricity, are incorporated in the analyses, capturing important strategies of plant resource-acquisition. However, other ecologically relevant traits, such as leaf phosphorus content, chlorophyll concentration, maximum carboxylation capacity

(Vcmax), wood density, and plant height, are not explicitly represented here, introducing uncertainties to map regional LUE variations. Adequate implementations of multiple plant traits, as well as their interactions with climatic factors and with themselves, should be addressed in the further study.

Alternatively, although the full model reproduces the tower-based LUE reasonably well, its prediction accuracy decreases towards the upper end of the LUE range. Similar underestimation of high productivity has been reported in many previous studies, partly because high-productivity ecosystems are often underrepresented in the observational datasets and partly because important physiological controls remain insufficiently characterized (Jung et al., 2011; Tramontana et al., 2016). The omission of key physiological traits and the limited availability of tower observations from highly productive ecosystems may therefore lead to the underestimation of peak LUE values in this study.

Additional uncertainty arises from the spatial representativeness of flux-tower observations. Although the flux sites used in this study encompass major ecosystem types across China, they cannot fully capture the environmental and ecological complexity of the entire region (Jung et al., 2011; Tramontana et al., 2016). The spatial distribution of the 29 flux tower sites is uneven across China, with varying number of sites over different PFTs. The limited number of sites for some PFTs may not fully capture the characteristics of LUE within those ecosystem types. Similarly, the uneven spatial distributions of flux tower observations may limit the performance of resulted regional-scale LUE representations. Further study with more even distributed flux tower observations with relatively longer time period are needed to improve our understanding of regional LUE variations. Furthermore, the trait datasets employed here were derived from spatially interpolated products that may not fully capture site-level variability (Van Bodegom et al., 2012). These uncertainties inevitably propagate into regional extrapolations and should be considered when interpreting the spatial distribution of LUE. In addition, the trait datasets show limited spatial coverage of leaf nitrogen content (N) and specific leaf area (SLA) data over croplands, causing the exclusion of cropland LUE in the analyses of this study. Such exclusion could induce limitations in the resulted regional LUE estimates as they do not fully represent LUE characteristics for agricultural ecosystems across China, and the extent to which croplands contribute to regional LUE variability and long-term trends remains uncertain. Future studies incorporating enough cropland flux tower observations and spatially consistent trait datasets are highly encouraged.

Another source of uncertainty relates to the temporal extrapolation of the RF model. Atmospheric $CO_2$ concentrations is increasing, and elevated $CO_2$ can directly stimulate photosynthetic carbon assimilation by enhancing Rubisco carboxylation and suppressing photorespiration, thereby affecting photosynthetic LUE (Ainsworth and Long, 2005; Kang et al., 2025). A global flux-tower analysis identifies $CO_2$ fertilization as an important contributor to temporal variations in ecosystem LUE (Liu et al., 2024). However, atmospheric $CO_2$ concentration is not included as a predictor in our RF model, introducing uncertainties into the magnitude of the estimated long-term LUE trend and hence future LUE predictions. Moreover, $CO_2$ responses vary among plant functional types and different environmental conditions (Ainsworth and Long, 2005). Future studies could incorporate atmospheric $CO_2$ concentrations or a physiologically based $CO_2$-response function into the upscaling framework to better constrain long-term LUE dynamics.

Despite these limitations, this study provides important implications for regional carbon-cycle model improvements. LUE is a key parameter linking absorbed radiation to carbon uptake and therefore directly influences estimates of gross primary productivity (GPP) and terrestrial carbon sinks (Monteith, 1972). By identifying the dominant roles of plant functional traits, vegetation type, and atmospheric water constraints in regulating LUE, this study contributes to a more ecologically informed understanding of ecosystem LUE across China. The investigations of the underlying mechanisms and the resultant regional LUE dataset provide a useful basis for improving carbon-cycle assessments, reducing uncertainties in terrestrial carbon uptake estimation and supporting accurate evaluations of ecosystem contributions to China's carbon-neutrality goals. More broadly, these findings highlight the value of integrating plant functional information into large-scale assessments of ecosystem functioning, thereby helping bridge the gap between plant ecological strategies and regional carbon-cycle dynamics.

## 4 Conclusions

Through integrating observations from 29 flux tower sites, this study investigates the spatial variations and the associated drivers of LUE across different ecosystems over China. The tower-based LUE is about $0.88 \pm 0.62$ g C $MJ^{-1}$, predominately driven by SLA × rooting depth, TA × SLA, SLA, VPD and VPD × SLA. PFT and isohydricity also evolve to influence LUE spatial variations in the study domain. Our results indicate that LUE is not governed by climate alone, but regulated by complex nonlinear interactions between climatic conditions and plant functional traits, with such interactions playing a dominant role over individual predictors. Based on the tower-related analyses, the regional LUE is mapping from 2003 to 2024, revealing non-significant temporal variations, but showing large spatial divergence. Overall, this study highlights the critical role of plant functional traits in constraining LUE and establishes a scalable, interpretable framework for advancing trait-based carbon cycle modeling at regional scales.

## Data availability

The eddy covariance data used in this study were obtained from ChinaFLUX, FLUXNET2015, and the post-processed carbon flux dataset for the Heihe River Basin. The remote-sensing, climatic, and plant functional trait datasets are available from the sources cited in Sect. 2.2. The processed data supporting the findings of this study are archived in Figshare and are available to editors and reviewers through the following private link: https://figshare.com/s/eedf7c05318b2480b90c. The repository will be made publicly available and assigned a DOI upon acceptance of the manuscript.

**Author contribution**

YW: data collection and processing, methodology, software, formal analysis, visualization, and writing - original draft. MH: conceptualization, supervision, funding acquisition, and writing - review and editing. QZ: validation, and writing - review and editing. All authors contributed to the interpretation of the results and approved the final version of the manuscript.

**Competing interests**

The authors declare that they have no conflict of interest.

**Financial support**

This work was supported by the National Natural Science Foundation of China

(Grant 42471114), the Taishan Scholars Program (Grant tsqn202306210), and the

Fundamental Research Funds for the Central Universities.

**References**

Ainsworth, E. A. and Long, S. P.: What have we learned from 15 years of free-air CO2 enrichment (FACE)? A meta-analytic review of the responses of photosynthesis, canopy properties and plant production to rising CO2, New Phytol., 165, 351–372, https://doi.org/10.1111/j.1469-8137.2004.01224.x, 2005.

Ali, A. A., Xu, C., Rogers, A., McDowell, N. G., Medlyn, B. E., Fisher, R. A., Wullschleger, S. D., Reich, P. B., Vrugt, J. A., Bauerle, W. L., Santiago, L. S., and Wilson, C. J.: Global-scale environmental control of plant photosynthetic capacity, Ecol. Appl., 25, 2349–2365, https://doi.org/10.1890/14-2111.1, 2015.

Allen, R. G., Pereira, L. S., Raes, D., and Smith, M.: Crop evapotranspiration: Guidelines for computing crop water requirements, FAO Irrigation and Drainage Paper No. 56, Food and Agriculture Organization of the United Nations, 1998.

An, N., Lu, N., Chen, W., Chen, Y., Shi, H., Wu, F., and Fu, B.: Spatial mapping of key plant functional traits in terrestrial ecosystems across China, Earth Syst. Sci. Data, 16, 1771–1810, https://doi.org/10.5194/essd-16-1771-2024, 2024.

Beer, C., Reichstein, M., Tomelleri, E., Ciais, P., Jung, M., Carvalhais, N., Rödenbeck, C., Arain, M. A., Baldocchi, D., Bonan, G. B., Bondeau, A., Cescatti, A., Lasslop, G., Lindroth, A., Lomas, M., Luyssaert, S., Margolis, H., Oleson, K. W., Roupsard, O., Veenendaal, E., Viovy, N., Williams, C., Woodward, F. I., and Papale, D.: Terrestrial gross carbon dioxide uptake: Global distribution and covariation with climate, Science, 329, 834–838, https://doi.org/10.1126/science.1184984, 2010.

Breiman, L.: Random forests, Mach. Learn., 45, 5–32, https://doi.org/10.1023/A:1010933404324, 2001.

Díaz, S., Kattge, J., Cornelissen, J. H. C., Wright, I. J., Lavorel, S., Dray, S., Reu, B., Kleyer, M., Wirth, C., Colin Prentice, I., Garnier, E., Bönisch, G., Westoby, M., Poorter, H., Reich, P. B., Moles, A. T., Dickie, J., Gillison, A. N., Zanne, A. E., Chave, J., Joseph Wright, S., Sheremet'ev, S. N., Jactel, H., Baraloto, C., Cerabolini, B., Pierce, S., Shipley, B., Kirkup, D., Casanoves,

F., Joswig, J. S., Günther, A., Falczuk, V., Rüger, N., Mahecha, M. D., and Gorné, L. D.: The global spectrum of plant form and function, Nature, 529, 167–171, https://doi.org/10.1038/nature16489, 2016.

Duan, H., Xue, X., Wang, T., Kang, W., Liao, J., and Liu, S.: Spatial and temporal differences in alpine meadow, alpine steppe and all vegetation of the Qinghai–Tibetan Plateau and their responses to climate change, Remote Sens., 13, 669, https://doi.org/10.3390/rs13040669, 2021.

Duffy, K. A., Schwalm, C. R., Arcus, V. L., Koch, G. W., Liang, L. L., and Schipper, L. A.: How close are we to the temperature tipping point of the terrestrial biosphere?, Sci. Adv., 7, eaay1052, https://doi.org/10.1126/sciadv.aay1052, 2021.

Durand, M., Stangl, Z. R., Salmon, Y., Burgess, A. J., Murchie, E. H., and Robson, T. M.: Sunflecks in the upper canopy: dynamics of light-use efficiency in sun and shade leaves of Fagus sylvatica, New Phytol., 235, 1365–1378, https://doi.org/10.1111/nph.18222, 2022.

Evans, J. R.: Photosynthesis and nitrogen relationships in leaves of C3 plants, Oecologia, 78, 9–19, https://doi.org/10.1007/BF00377192, 1989.

Fan, Y., Miguez-Macho, G., Jobbágy, E. G., Jackson, R. B., and Otero-Casal, C.: Hydrologic regulation of plant rooting depth, Proc. Natl. Acad. Sci., 114, 10572–10577, https://doi.org/10.1073/pnas.1712381114, 2017.

Fang, J., Bowman, K., Zhao, W., Lian, X., and Gentine, P.: Differentiable land model reveals global environmental controls on ecological parameters, https://doi.org/10.48550/ARXIV.2411.09654, 2024., 2024.

Fei, X.-H., Song, Q.-H., Zhang, Y.-P., Yu, G.-R., Zhang, L.-M., Sha, L.-Q., Liu, Y.-T., Xu, K., Chen, H., Wu, C.-S., Chen, A.-G., Zhang, S.-B., Liu, W.-W., Huang, H., Deng, Y., Qin, H.-L., Li, P.-G., and Grace, J.: Patterns and Controls of Light Use Efficiency in Four Contrasting Forest Ecosystems in Yunnan, Southwest China, J. Geophys. Res. Biogeosciences, 124, 293–311, https://doi.org/10.1029/2018JG004487, 2019.

Friedlingstein, P., O'Sullivan, M., Jones, M. W., Andrew, R. M., Bakker, D. C. E., Hauck, J., Landschützer, P., Le Quéré, C., Luijkx, I. T., Peters, G. P., Peters, W., Pongratz, J., Schwingshackl, C., Sitch, S., Canadell, J. G., Ciais, P., Jackson, R. B., Alin, S. R., Anthoni, P., Barbero, L., Bates, N. R., Becker, M., Bellouin, N., Decharme, B., Bopp, L., Brasika, I. B. M., Cadule, P., Chamberlain, M. A., Chandra, N., Chau, T.-T.-T., Chevallier, F., Chini, L. P., Cronin, M., Dou, X., Enyo, K., Evans, W., Falk, S., Feely, R. A., Feng, L., Ford, D. J., Gasser, T., Ghattas, J., Gkritzalis, T., Grassi, G., Gregor, L., Gruber, N., Gürses, Ö., Harris, I., Hefner, M., Heinke, J., Houghton, R. A., Hurtt, G. C., Iida, Y., Ilyina, T., Jacobson, A. R., Jain, A., Jarníková, T., Jersild, A., Jiang, F., Jin, Z., Joos, F., Kato, E., Keeling, R. F., Kennedy, D., Klein Goldewijk, K., Knauer, J., Korsbakken, J. I., Körtzinger, A., Lan, X., Lefèvre, N., Li, H., Liu, J., Liu, Z., Ma, L., Marland, G., Mayot, N., McGuire, P. C., McKinley, G. A., Meyer, G., Morgan, E. J., Munro, D. R., Nakaoka, S.-I., Niwa, Y., O'Brien, K. M., Olsen, A., Omar, A. M., Ono, T., Paulsen, M., Pierrot, D., Pocock, K., Poulter, B., Powis, C. M., Rehder, G., Resplandy, L., Robertson, E., Rödenbeck, C., Rosan, T. M., Schwinger, J., Séférian, R., Smallman, T. L., Smith, S. M., Sospedra-Alfonso, R., Sun, Q., Sutton, A. J., Sweeney, C., Takao, S., Tans, P. P., Tian, H., Tilbrook, B., Tsujino, H., Tubiello, F., Van Der Werf, G. R., Van Ooijen, E., Wanninkhof, R., Watanabe, M., Wimart-Rousseau, C., Yang, D., Yang, X., Yuan, W., Yue, X., Zaehle, S., Zeng, J., and Zheng, B.: Global carbon budget 2023, Earth Syst. Sci. Data, 15, 5301–5369, https://doi.org/10.5194/essd-15-5301-2023, 2023.

Ganjurjav, H., Gao, Q., Gornish, E. S., Schwartz, M. W., Liang, Y., Cao, X., Zhang, W., Zhang, Y., Li, W., Wan, Y., Li, Y., Danjiu, L., Guo, H., and Lin, E.: Differential response of alpine steppe and alpine meadow to climate warming in the central Qinghai–Tibetan Plateau, Agric. For. Meteorol., 223, 233–240, https://doi.org/10.1016/j.agrformet.2016.03.017, 2016.

Garbulsky, M. F., Peñuelas, J., Papale, D., Ardö, J., Goulden, M. L., Kiely, G., Richardson, A. D., Rotenberg, E., Veenendaal, E. M., and Filella, I.: Patterns and controls of the variability of radiation use efficiency and primary productivity across terrestrial ecosystems, Glob. Ecol. Biogeogr., 19, 253–267, https://doi.org/10.1111/j.1466-8238.2009.00504.x, 2010.

Golivets, M., Knapp, S., Essl, F., Lenzner, B., Latombe, G., Leung, B., and Kühn, I.: Future changes in key plant traits across Central Europe vary with biogeographical status, woodiness, and habitat type, Sci. Total Environ., 907, 167954, https://doi.org/10.1016/j.scitotenv.2023.167954, 2024.

Grossiord, C., Buckley, T. N., Cernusak, L. A., Novick, K. A., Poulter, B., Siegwolf, R. T. W., Sperry, J. S., and McDowell, N. G.: Plant responses to rising vapor pressure deficit, New Phytol., 226, 1550–1566, https://doi.org/10.1111/nph.16485, 2020.

Hao, A., Duan, H., Wang, X., Zhao, G., You, Q., Peng, F., Du, H., Liu, F., Li, C., Lai, C., and Xue, X.: Different response of alpine meadow and alpine steppe to climatic and anthropogenic disturbance on the Qinghai-Tibetan Plateau, Glob. Ecol. Conserv., 27, e01512, https://doi.org/10.1016/j.gecco.2021.e01512, 2021.

He, M., Chen, S., Lian, X., Wang, X., Peñuelas, J., and Piao, S.: Global spectrum of vegetation light-use efficiency, Geophys. Res. Lett., 49, e2022GL099550, https://doi.org/10.1029/2022GL099550, 2022.

Heinsch, F. A., Zhao, M., Running, S. W., Kimball, J. S., Nemani, R. R., Davis, K. J., Bolstad, P. V., Cook, B. D., Desai, A. R., Ricciuto, D. M., Law, B. E., Oechel, W. C., Kwon, H., Luo, H., Wofsy, S. C., Dunn, A. L., Munger, J. W., Baldocchi, D. D., Xu, L., Hollinger, D. Y., Richardson, A. D., Stoy, P. C., Siqueira, M. B. S., Monson, R. K., Burns, S. P., and Flanagan, L. B.: Evaluation of remote sensing based terrestrial productivity from MODIS using regional tower eddy flux network observations, IEEE Trans. Geosci. Remote Sens., 44, 1908–1925, https://doi.org/10.1109/TGRS.2005.853936, 2006.

Hua, R., Zhang, P., Wang, L., Huang, M., Hua, L., and Zhou, J.: Alpine steppe vegetation communities are more sensitive to plateau pika disturbance than alpine meadows, Front. Plant Sci., 16, 1546828, https://doi.org/10.3389/fpls.2025.1546828, 2025-5-29.

Humphrey, V., Berg, A., Ciais, P., Gentine, P., Jung, M., Reichstein, M., Seneviratne, S. I., and Frankenberg, C.: Soil moisture–atmosphere feedback dominates land carbon uptake variability, Nature, 592, 65–69, https://doi.org/10.1038/s41586-021-03325-5, 2021.

Jung, M., Reichstein, M., Margolis, H. A., Cescatti, A., Richardson, A. D., Arain, M. A., Arneth, A., Bernhofer, C., Bonal, D., Chen, J., Gianelle, D., Gobron, N., Kiely, G., Kutsch, W., Lasslop, G., Law, B. E., Lindroth, A., Merbold, L., Montagnani, L., Moors, E. J., Papale, D., Sottocornola, M., Vaccari, F., and Williams, C.: Global patterns of land-atmosphere fluxes of carbon dioxide, latent heat, and sensible heat derived from eddy covariance, satellite, and meteorological observations, J. Geophys. Res. Biogeosciences, 116, https://doi.org/10.1029/2010JG001566, 2011.

Kang, Y., Bassiouni, M., Gaber, M., Lu, X., and Keenan, T. F.: CEDAR-GPP: spatiotemporally upscaled estimates of gross primary productivity incorporating $CO_2$ fertilization, Earth Syst. Sci. Data, 17, 3009–3046, https://doi.org/10.5194/essd-17-3009-2025, 2025.

Konings, A. G. and Gentine, P.: Global variations in ecosystem-scale isohydricity, Glob. Change Biol., 23, 891–905, https://doi.org/10.1111/gcb.13389, 2017.

Lin, S., Li, J., Liu, Q., Gioli, B., Paul-Limoges, E., Buchmann, N., Gharun, M., Hörtnagl, L., Foltýnová, L., Dušek, J., Li, L., and Yuan, W.: Improved global estimations of gross primary productivity of natural vegetation types by incorporating plant functional type, Int. J. Appl. Earth Obs. Geoinformation, 100, 102328, https://doi.org/10.1016/j.jag.2021.102328, 2021.

Liu, Z., He, C., Xu, J., Sun, H., Dai, X., Cui, E., Qiu, C., Xia, J., and Huang, K.: Observed increasing light-use efficiency of terrestrial gross primary productivity, Agric. For. Meteorol., 359, 110269, https://doi.org/10.1016/j.agrformet.2024.110269, 2024.

Lundberg, S. and Lee, S.-I.: A unified approach to interpreting model predictions, https://doi.org/10.48550/ARXIV.1705.07874, 2017., 2017.

Lusk, D., Wolf, S., Svidzinska, D., Dormann, C. F., Kattge, J., Bruelheide, H., Sabatini, F. M., Damasceno, G., Moreno Martínez, Á., Violle, C., Hending, D., Hähn, G. J. A., Tabeni, S., Phartyal, S., Gonçalves, F., Kreft, H., Schmidt, M., Chen, H., Güler, B., Dolezal, J., Pielech, R., Guido, A., Dwyer, C., Napoleone, F., Willie, J., Gasper, A. L., Macía, M. J., Chytry, M., Lenoir, J., Thakur, D., Dengler, J., Świerszcz, S., Altman, J., Mucina, L., Nerlekar, A. N., Kakinuma, K., Rawat, P., Stančić, Z., Testolin, R., Hatim, M. Z., Rodrigues, F., Homeier, J., Marques, M. C. M., McCarthy, J. K., El-Sheikh, M. A., Korznikov, K., Gerberding, K., and Kattenborn, T.: Crowdsourced biodiversity monitoring fills gaps in global plant trait mapping, Nat. Commun., 17, 1203, https://doi.org/10.1038/s41467-026-68996-y, 2026.

Madani, N., Kimball, J. S., and Running, S. W.: Improving global gross primary productivity estimates by computing optimum light use efficiencies using flux tower data, J. Geophys. Res. Biogeosciences, 122, 2939–2951, https://doi.org/10.1002/2017JG004142, 2017.

Matheny, A. M., Mirfenderesgi, G., and Bohrer, G.: Trait-based representation of hydrological functional properties of plants in weather and ecosystem models, Plant Divers., 39, 1–12, https://doi.org/10.1016/j.pld.2016.10.001, 2017.

Mei, L., Bao, G., Tong, S., Yin, S., Bao, Y., Jiang, K., Hong, Y., Tuya, A., and Huang, X.: Elevation-dependent response of spring phenology to climate and its legacy effect on vegetation growth in the mountains of northwest Mongolia, Ecol. Indic., 126, 107640, https://doi.org/10.1016/j.ecolind.2021.107640, 2021.

Monteith, J. L.: Solar radiation and productivity in tropical ecosystems, J. Appl. Ecol., 9, 747–766, https://doi.org/10.2307/2401901, 1972.

Muñoz-Sabater, J., Dutra, E., Agustí-Panareda, A., Albergel, C., Arduini, G., Balsamo, G., Boussetta, S., Choulga, M., Harrigan, S., Hersbach, H., Martens, B., Miralles, D. G., Piles, M., Rodríguez-Fernández, N. J., Zsoter, E., Buontempo, C., and Thépaut, J.-N.: ERA5-Land: a state-of-the-art global reanalysis dataset for land applications, Earth Syst. Sci. Data, 13, 4349–4383, https://doi.org/10.5194/essd-13-4349-2021, 2021.

Myneni, R., Knyazikhin, Y., and Park, T.: MODIS/Terra Leaf Area Index/FPAR 8-Day L4 Global 500m SIN Grid V061, https://doi.org/10.5067/MODIS/MOD15A2H.061, 2021.

Ni, J.: Forage yield-based carbon storage in grasslands of China, Clim. Change, 67, 237–246, https://doi.org/10.1007/s10584-004-0070-8, 2004.

Novick, K. A., Oishi, A. C., and Miniat, C. F.: Cold air drainage flows subsidize montane valley ecosystem productivity, Glob. Change Biol., 22, 4014–4027, https://doi.org/10.1111/gcb.13320, 2016.

Novick, K. A., Ficklin, D. L., Grossiord, C., Konings, A. G., Martínez-Vilalta, J., Sadok, W., Trugman, A. T., Williams, A. P., Wright, A. J., Abatzoglou, J. T., Dannenberg, M. P., Gentine, P., Guan, K., Johnston, M. R., Lowman, L. E. L., Moore, D. J. P., and McDowell, N. G.: The impacts of rising vapour pressure deficit in natural and managed ecosystems, Plant Cell Environ., 47, 3561–3589, https://doi.org/10.1111/pce.14846, 2024.

Pastorello, G., Trotta, C., Canfora, E., Chu, H., Christianson, D., Cheah, Y.-W., Poindexter, C., Chen, J., Elbashandy, A., Humphrey, M., Isaac, P., Polidori, D., Reichstein, M., Ribeca, A., van Ingen, C., Vuichard, N., Zhang, L., Amiro, B., Ammann, C., Arain, M. A., Ardö, J., Arkebauer, T., Arndt, S. K., Arriga, N., Aubinet, M., Aurela, M., Baldocchi, D., Barr, A., Beamesderfer, E., Marchesini, L. B., Bergeron, O., Beringer, J., Bernhofer, C., Berveiller, D., Billesbach, D., Black, T. A., Blanken, P. D., Bohrer, G., Boike, J., Bolstad, P. V., Bonal, D., Bonnefond, J.-M., Bowling, D. R., Bracho, R., Brodeur, J., Brümmer, C., Buchmann, N., Burban, B., Burns, S. P., Buysse, P., Cale, P., Cavagna, M., Cellier, P., Chen, S., Chini, I.,

Christensen, T. R., Cleverly, J., Collalti, A., Consalvo, C., Cook, B. D., Cook, D., Coursolle, C., Cremonese, E., Curtis, P. S., D'Andrea, E., da Rocha, H., Dai, X., Davis, K. J., Cinti, B. D., Grandcourt, A. de, Ligne, A. D., De Oliveira, R. C., Delpierre, N., Desai, A. R., Di Bella, C. M., Tommasi, P. di, Dolman, H., Domingo, F., Dong, G., Dore, S., Duce, P., Dufrêne, E., Dunn, A., Dušek, J., Eamus, D., Eichelmann, U., ElKhidir, H. A. M., Eugster, W., Ewenz, C. M., Ewers, B., Famulari, D., Fares, S., Feigenwinter, I., Feitz, A., Fensholt, R., Filippa, G., Fischer, M., Frank, J., Galvagno, M., Gharun, M., Gianelle, D., Gielen, B., Gioli, B., Gitelson, A., Goded, I., Goeckede, M., Goldstein, A. H., Gough, C. M., Goulden, M. L., Graf, A., Griebel, A., Gruening, C., Grünwald, T., Hammerle, A., Han, S., Han, X., Hansen, B. U., Hanson, C., Hatakka, J., He, Y., Hehn, M., Heinesch, B., Hinko-Najera, N., Hörtnagl, L., Hutley, L., Ibrom, A., Ikawa, H., Jackowicz-Korczynski, M., Janouš, D., Jans, W., Jassal, R., Jiang, S., Kato, T., Khomik, M., Klatt, J., Knohl, A., Knox, S., Kobayashi, H., Koerber, G., Kolle, O., Kosugi, Y., Kotani, A., Kowalski, A., Kruijt, B., Kurbatova, J., Kutsch, W. L., Kwon, H., Launiainen, S., Laurila, T., Law, B., Leuning, R., Li, Y., Liddell, M., Limousin, J.-M., Lion, M., Liska, A. J., Lohila, A., López-Ballesteros, A., López-Blanco, E., Loubet, B., Loustau, D., Lucas-Moffat, A., Lüers, J., Ma, S., Macfarlane, C., Magliulo, V., Maier, R., Mammarella, I., Manca, G., Marcolla, B., Margolis, H. A., Marras, S., Massman, W., Mastepanov, M., Matamala, R., Matthes, J. H., Mazzenga, F., McCaughey, H., McHugh, I., McMillan, A. M. S., Merbold, L., Meyer, W., Meyers, T., Miller, S. D., Minerbi, S., Moderow, U., Monson, R. K., Montagnani, L., Moore, C. E., Moors, E., Moreaux, V., Moureaux, C., Munger, J. W., Nakai, T., Neirynck, J., Nesic, Z., Nicolini, G., Noormets, A., Northwood, M., Nosetto, M., Nouvellon, Y., Novick, K., Oechel, W., Olesen, J. E., Ourcival, J.-M., Papuga, S. A., Parmentier, F.-J., Paul-Limoges, E., Pavelka, M., Peichl, M., Pendall, E., Phillips, R. P., Pilegaard, K., Pirk, N., Posse, G., Powell, T., Prasse, H., Prober, S. M., Rambal, S., Rannik, Ü., Raz-Yaseef, N., Rebmann, C., Reed, D., Dios, V. R. de, Restrepo-Coupe, N., Reverter, B. R., Roland, M., Sabbatini, S., Sachs, T., Saleska, S. R., Sánchez-Cañete, E. P., Sanchez-Mejia, Z. M., Schmid, H. P., Schmidt, M., Schneider, K., Schrader, F., Schroder, I., Scott, R. L., Sedlák, P., Serrano-Ortíz, P., Shao, C., Shi, P., Shironya, I., Siebicke, L., Šigut, L., Silberstein, R., Sirca, C., Spano, D., Steinbrecher, R., Stevens, R. M., Sturtevant, C., Suyker, A., Tagesson, T., Takanashi, S., Tang, Y., Tapper, N., Thom, J., Tomassucci, M., Tuovinen, J.-P., Urbanski, S., Valentini, R., van der Molen, M., van Gorsel, E., van Huissteden, K., Varlagin, A., Verfaillie, J., Vesala, T., Vincke, C., Vitale, D., Vygodskaya, N., Walker, J. P., Walter-Shea, E., Wang, H., Weber, R., Westermann, S., Wille, C., Wofsy, S., Wohlfahrt, G., Wolf, S., Woodgate, W., Li, Y., Zampedri, R., Zhang, J., Zhou, G., Zona, D., Agarwal, D., Biraud, S., Torn, M., and Papale, D.: The FLUXNET2015 dataset and the ONEFlux processing pipeline for eddy covariance data, Sci. Data, 7, 225, https://doi.org/10.1038/s41597-020-0534-3, 2020.

Pei, Y., Dong, J., Zhang, Y., Yuan, W., Doughty, R., Yang, J., Zhou, D., Zhang, L., and Xiao, X.: Evolution of light use efficiency models: Improvement, uncertainties, and implications, Agric. For. Meteorol., 317, 108905, https://doi.org/10.1016/j.agrformet.2022.108905, 2022.

Peng, S., Ding, Y., Liu, W., and Li, Z.: 1 km monthly temperature and precipitation dataset for China from 1901 to 2017, Earth Syst. Sci. Data, 11, 1931–1946, https://doi.org/10.5194/essd-11-1931-2019, 2019.

Piao, S., Ciais, P., Huang, Y., Shen, Z., Peng, S., Li, J., Zhou, L., Liu, H., Ma, Y., Ding, Y., Friedlingstein, P., Liu, C., Tan, K., Yu, Y., Zhang, T., and Fang, J.: The impacts of climate change on water resources and agriculture in China, Nature, 467, 43–51, https://doi.org/10.1038/nature09364, 2010.

Reich, P. B.: The world-wide 'fast–slow' plant economics spectrum: a traits manifesto, J. Ecol., 102, 275–301, https://doi.org/10.1111/1365-2745.12211, 2014.

Rogers, A., Medlyn, B. E., Dukes, J. S., Bonan, G., Von Caemmerer, S., Dietze, M. C., Kattge, J., Leakey, A. D. B., Mercado, L. M., Niinemets, Ü., Prentice, I. C., Serbin, S. P., Sitch, S., Way, D. A., and Zaehle, S.: A roadmap for improving the representation of photosynthesis in Earth system models, New Phytol., 213, 22–42, https://doi.org/10.1111/nph.14283, 2017.

Running, S. W., Nemani, R. R., Heinsch, F. A., Zhao, M., Reeves, M., and Hashimoto, H.: A Continuous Satellite-Derived Measure of Global Terrestrial Primary Production, BioScience, 54, 547–560, https://doi.org/10.1641/0006-3568(2004)054%5B0547:ACSMOG%5D2.0.CO;2, 2004.

Shen, M., Wang, S., Jiang, N., Sun, J., Cao, R., Ling, X., Fang, B., Zhang, L., Zhang, L., Xu, X., Lv, W., Li, B., Sun, Q., Meng, F., Jiang, Y., Dorji, T., Fu, Y., Iler, A., Vitasse, Y., Steltzer, H., Ji, Z., Zhao, W., Piao, S., and Fu, B.: Plant phenology changes and drivers on the Qinghai–Tibetan Plateau, Nat. Rev. Earth Environ., 3, 633–651, https://doi.org/10.1038/s43017-022-00317-5, 2022.

Song, P., Zhang, Y., Guo, J., Shi, J., Zhao, T., and Tong, B.: A 1 km daily surface soil moisture dataset of enhanced coverage under all-weather conditions over China in 2003–2019, Earth Syst. Sci. Data, 14, 2613–2637, https://doi.org/10.5194/essd-14-2613-2022, 2022.

Tang, S., Wang, X., He, M., Huang, L., Zhang, Y., Yang, H., and Piao, S.: Global patterns and climate controls of terrestrial ecosystem light use efficiency, J. Geophys. Res. Biogeosciences, 125, e2020JG005908, https://doi.org/10.1029/2020JG005908, 2020.

Tardieu, F. and Simonneau, T.: Variability among species of stomatal control under fluctuating soil water status and evaporative demand: modelling isohydric and anisohydric behaviours, J. Exp. Bot., 49, 419–432, https://doi.org/10.1093/jxb/49.Special_Issue.419, 1998.

Tramontana, G., Jung, M., Schwalm, C. R., Ichii, K., Camps-Valls, G., Ráduly, B., Reichstein, M., Arain, M. A., Cescatti, A., Kiely, G., Merbold, L., Serrano-Ortiz, P., Sickert, S., Wolf, S., and Papale, D.: Predicting carbon dioxide and energy fluxes across global FLUXNET sites with regression algorithms, Biogeosciences, 13, 4291–4313, https://doi.org/10.5194/bg-13-4291-2016, 2016.

Van Bodegom, P. M., Douma, J. C., Witte, J. P. M., Ordoñez, J. C., Bartholomeus, R. P., and Aerts, R.: Going beyond limitations of plant functional types when predicting global ecosystem–atmosphere fluxes: exploring the merits of traits-based approaches, Glob. Ecol. Biogeogr., 21, 625–636, https://doi.org/10.1111/j.1466-8238.2011.00717.x, 2012.

Verheijen, L. M., Aerts, R., Brovkin, V., Cavender-Bares, J., Cornelissen, J. H. C., Kattge, J., and van Bodegom, P. M.: Inclusion of ecologically based trait variation in plant functional types reduces the projected land carbon sink in an earth system model, Glob. Change Biol., 21, 3074–3086, https://doi.org/10.1111/gcb.12871, 2015.

Walker, A. P., Beckerman, A. P., Gu, L., Kattge, J., Cernusak, L. A., Domingues, T. F., Scales, J. C., Wohlfahrt, G., Wullschleger, S. D., and Woodward, F. I.: The relationship of leaf photosynthetic traits – Vcmax and Jmax – to leaf nitrogen, leaf phosphorus, and specific leaf area: a meta-analysis and modeling study, Ecol. Evol., 4, 3218–3235, https://doi.org/10.1002/ece3.1173, 2014.

Wang, D.: MODIS/Terra+Aqua Photosynthetically Active Radiation Daily/3-Hour L3 Global 0.05Deg CMG V062 | NASA Earthdata, https://www.earthdata.nasa.gov/data/catalog/lpcloud-mcd18c2-062 (last access: 10 October 2026), 2025.

Wang, X., Che, T., Xiao, J., Wang, T., Tan, J., Zhang, Y., Ren, Z., Geng, L., Wang, H., Xu, Z., Liu, S., and Li, X.: A post-processed carbon flux dataset for 34 eddy covariance flux sites across the Heihe River basin, China, Earth Syst. Sci. Data, 17, 1329–1346, https://doi.org/10.5194/essd-17-1329-2025, 2025.

Wright, I. J., Reich, P. B., Westoby, M., Ackerly, D. D., Baruch, Z., Bongers, F., Cavender-Bares, J., Chapin, T., Cornelissen, J. H. C., Diemer, M., Flexas, J., Garnier, E., Groom, P. K., Gulias, J., Hikosaka, K., Lamont, B. B., Lee, T., Lee, W., Lusk, C., Midgley, J. J., Navas, M.-L., Niinemets, Ü., Oleksyn, J., Osada, N., Poorter, H., Poot, P., Prior, L., Pyankov, V. I., Roumet, C., Thomas, S. C., Tjoelker, M. G., Veneklaas, E. J., and Villar, R.: The worldwide leaf economics spectrum, Nature, 428, 821–827, https://doi.org/10.1038/nature02403, 2004.

Xie, J., Yin, G., Ma, D., Chen, R., Zhao, W., Xie, Q., Wang, C., Lin, S., and Yuan, W.: Climatic limitations on grassland photosynthesis over the Tibetan Plateau shifted from temperature to water, Sci. Total Environ., 906, 167663, https://doi.org/10.1016/j.scitotenv.2023.167663, 2024.

Yan, Y., Li, B., Dechant, B., Xu, M., Luo, X., Qu, S., Miao, G., Leng, J., Shang, R., Shu, L., Jiang, C., Wang, H., Jeong, S., Ryu, Y., and Chen, J. M.: Plant traits shape global spatiotemporal variations in photosynthetic efficiency, Nat. Plants, 11, 924–934, https://doi.org/10.1038/s41477-025-01958-2, 2025.

Yang, W.-S., Liu, Y., Zhao, J., Chang, X., Wiesmeier, M., Sun, J., López-Vicente, M., García-Ruiz, R., Gómez, J. A., Zhou, H., Shi, J., and Wu, G.-L.: SOC changes were more sensitive in alpine grasslands than in temperate grasslands during grassland transformation in China: A meta-analysis, J. Clean. Prod., 308, 127430, https://doi.org/10.1016/j.jclepro.2021.127430, 2021.

Yang, X., Tang, J., Mustard, J. F., Lee, J.-E., Rossini, M., Joiner, J., Munger, J. W., Kornfeld, A., and Richardson, A. D.: Solar-induced chlorophyll fluorescence that correlates with canopy photosynthesis on diurnal and seasonal scales in a temperate deciduous forest, Geophys. Res. Lett., 42, 2977–2987, https://doi.org/10.1002/2015GL063201, 2015.

Yu, G.-R., Wen, X.-F., Sun, X.-M., Tanner, B. D., Lee, X., and Chen, J.-Y.: Overview of ChinaFLUX and evaluation of its eddy covariance measurement, Agric. For. Meteorol., 137, 125–137, https://doi.org/10.1016/j.agrformet.2006.02.011, 2006.

Yuan, W., Liu, S., Zhou, G., Zhou, G., Tieszen, L. L., Baldocchi, D., Bernhofer, C., Gholz, H., Goldstein, A. H., Goulden, M. L., Hollinger, D. Y., Hu, Y., Law, B. E., Stoy, P. C., Vesala, T., and Wofsy, S. C.: Deriving a light use efficiency model from eddy covariance flux data for predicting daily gross primary production across biomes, Agric. For. Meteorol., 143, 189–207, https://doi.org/10.1016/j.agrformet.2006.12.001, 2007.

Yuan, W., Liu, S., Yu, G., Bonnefond, J.-M., Chen, J., Davis, K., Desai, A. R., Goldstein, A. H., Gianelle, D., Rossi, F., Suyker, A. E., and Verma, S. B.: Global estimates of evapotranspiration and gross primary production based on MODIS and global meteorology data, Remote Sens. Environ., 114, 1416–1431, https://doi.org/10.1016/j.rse.2010.01.022, 2010.

Zhang, Y., Xiao, X., Wu, X., Zhou, S., Zhang, G., Qin, Y., and Dong, J.: A global moderate resolution dataset of gross primary production of vegetation for 2000–2016, Sci. Data, 4, 170165, https://doi.org/10.1038/sdata.2017.165, 2017.

Zhang, Y., Joiner, J., Alemohammad, S. H., Zhou, S., and Gentine, P.: A global spatially contiguous solar-induced fluorescence (CSIF) dataset using neural networks, Biogeosciences, 15, 5779–5800, https://doi.org/10.5194/bg-15-5779-2018, 2018.

Zhao, M., Heinsch, F. A., Nemani, R. R., and Running, S. W.: Improvements of the MODIS terrestrial gross and net primary production global data set, Remote Sens. Environ., 95, 164–176, https://doi.org/10.1016/j.rse.2004.12.011, 2005.

Zhou, L., Wang, S., Chi, Y., Li, Q., Huang, K., and Yu, Q.: Responses of photosynthetic parameters to drought in subtropical forest ecosystem of China, Sci. Rep., 5, 18254, https://doi.org/10.1038/srep18254, 2015.